JGR Biogeosciences

RESEARCH ARTICLE
10.1029/2021JG006242

Special Section:
Carbon Weather: Toward the next generation of regional greenhouse gas inversion systems

Sustained-Flux Global Warming Potential Driven by Nitrogen Inflow and Hydroperiod in a Model of Great Lakes Coastal Wetlands

Y. Yuan[1], S. J. Sharp[1], J. P. Martina[2], K. J. Elgersma[3], and W. S. Currie[1]

[1]School for Environment and Sustainability, University of Michigan, Ann Arbor, MI, USA, [2]Department of Biology, Texas State University, San Marcos, TX, USA, [3]Department of Biology, University of Northern Iowa, Cedar Falls, IA, USA

Key Points:

- Wetland methane emissions had a far greater effect on net sustained-flux global warming potential than carbon dioxide or nitrous oxide
- The positive net sustained-flux global warming potential was dominated by methane emission in our simulations
- Our study illustrated the strength of using a process-based model to reveal the interactions between drivers of greenhouse gas emissions

Supporting Information:

Supporting Information may be found in the online version of this article.

Correspondence to:
Y. Yuan,
yeyua@umich.edu

Citation:
Yuan, Y., Sharp, S. J., Martina, J. P., Elgersma, K. J., & Currie, W. S. (2021). Sustained-flux global warming potential driven by nitrogen inflow and hydroperiod in a model of Great Lakes coastal wetlands. *Journal of Geophysical Research: Biogeosciences*, *126*, e2021JG006242. https://doi.org/10.1029/2021JG006242

Received 5 JAN 2021
Accepted 26 JUL 2021

Abstract Wetlands impact global warming by regulating the atmospheric exchange of greenhouse gases (GHGs), including carbon dioxide (CO_2), methane (CH_4), and nitrous oxide (N_2O). We investigated GHG emissions in the Great Lakes coastal wetlands across various hydrologic, temperature, and nitrogen (N) inflow regimes using a process-based simulation model. We found the emission of CH_4, N_2O, and sequestration of C (i.e., negative net ecosystem exchange, NEE) in our simulations were all positively related to water residence time and N inflow, primarily due to greater plant productivity and N uptake, which facilitated greater C and N cycling rates in the model. Water level scenarios also had an effect on GHG exchanges by moderating the transitions between aerobic and anaerobic conditions. Temperature effects on GHGs were minimal compared with other factors. The net sustained-flux global warming potential (SGWP; i.e., sum SGWP of CH_4, N_2O, and NEE) of wetlands on 20-year and 100-year time horizons were both primarily driven by CH_4 emissions and strongly controlled by the tradeoffs between CH_4 emission and CO_2 sequestration, with a negligible amount of simulated N_2O emissions. Future research could include model enhancements to provide increased process-level details on the aerobic-anaerobic transitions or the direct effects of plants on mediating GHG exchanges. Field studies addressing the interaction of N inflows and water residence time at appropriately large scales are needed to test the complex interactions revealed by our modeling study. Our results highlight the previously under-appreciated role of nitrogen and water residence time in modulating SGWP in coastal wetlands.

Plain Language Summary Wetlands impact global warming by emitting carbon dioxide (CO_2), methane (CH_4), and nitrous oxide (N_2O) to the atmosphere, but can absorb these greenhouse gases (GHGs). In our study, we investigated GHG emission in the Great Lakes coastal wetlands under different hydrologic, temperature, and nitrogen (N) inflow regimes using a simulation ecosystem model. We found the emission of CH_4 and N_2O increased with longer water residence time and higher N inflow in our modeling results, but at the same time, more carbon was absorbed by wetlands because wetland plants produced more biomass with more nutrients. The summed sustained-flux global warming potential of wetlands on 20-year and 100-year time horizons both depend on if global warming potential caused by CH_4 could be offset by the negative global warming potential of CO_2.

1. Introduction

Global climate warming is one of the most serious environmental problems of our time and is mostly driven by increasing human-dominated emissions of greenhouse gases (GHGs) into the atmosphere (IPCC, 2013). Wetlands play a large role in regulating GHG emissions by storing and processing carbon (C) and nitrogen (N) (Beringer et al., 2013; IPCC, 2013; Mitsch & Gosselink, 2007, 2015; Song et al., 2009; Whiting & Chanton, 2001). Carbon dioxide (CO_2), methane (CH_4), and nitrous oxide (N_2O) are three key greenhouse gases (hereafter GHGs) that contribute to global warming and are associated with wetlands (Forster et al., 2007; IPCC, 2013). Wetland ecosystems produce much of the world's CH_4 and N_2O (Bridgham et al., 2013; Kirschke et al., 2013; Saunois et al., 2020; Xu et al., 2008), and also function as either sources or sinks of another GHG CO_2, as the balance of ecosystem respiration and plant CO_2 uptake (Beringer et al., 2013; Lu et al., 2017). The magnitude of GHG emissions from wetlands may be affected by climate change and human activities that have impacted wetlands in numerous ways, including changes in hydrology, temperature, and elevated

inflow of N (IPCC, 2013). Emissions of CH_4 and N_2O have more severe impacts per unit mass than CO_2 because the SGWPs of equal masses of CH_4 and N_2O are 45 and 270 times greater, respectively, than the contribution of CO_2 to global warming over a 100-year time horizon (Neubauer & Megonigal, 2015). We focus on these three GHGs in the present study, including comparisons of the sustained-flux global warming potentials (SGWPs) among the three.

Wetlands, which experience fluctuating water levels and associated alternating aerobic and anaerobic soil conditions, may exhibit high variability of GHG emissions. Previous studies have demonstrated that lowering the water table increased CO_2 emissions by increasing oxygen availability and accelerating organic matter decomposition (Blodau et al., 2004; Chimner & Cooper, 2003; Moore & Dalva, 1993; Yang et al., 2013). However, lower wetland water levels are also associated with lower net methane production due to either lower methanogenesis or greater methane oxidation in aerobic surface layers (Blodau & Moore, 2003; Dinsmore et al., 2009; Moore & Dalva, 1993). Emissions of N_2O are similarly affected by shifting aerobic and anaerobic conditions. More anaerobic soils can lead to a decrease in the proportion of denitrified N emitted as N_2O in wetlands because denitrifying microbes more completely reduce N_2O to N_2 in more anaerobic environments (Lohila et al., 2010; Yang et al., 2013).

Water residence time, another hydrologic variable, is an important driver of wetland GHG emissions that vary greatly among wetlands. Water residence time is an important component of N cycling because it defines how long water, and any solute (e.g., dissolved N), remains in a wetland. If water residence time is very short (i.e., water flushing rate is high), N in water flowing into the wetland does not remain long in the system but is flushed out quickly. Longer water residence time promotes more denitrification and N removal in simulation studies as N accumulates in wetlands (Sharp et al., 2020). In a membrane bioreactor experiment, as the hydraulic residence time reduced from 5 to 2.5 days, CH_4 and N_2O gas production levels significantly decreased (Nuansawan et al., 2016).

Nitrogen inflow is another known modulator of wetland GHG emissions, but how important it is and how N regulates wetland SGWP is still unclear. Many studies have focused on hydrology and N loading in regard to GHG emissions from wetlands, but the effect of their interaction is not well known. Nitrogen inflow affects CO_2 flux by increasing plant productivity, improving the chemical quality of litter (lower C/N ratio), and alleviating N constraints on microbial metabolism (LeBauer & Treseder, 2008). Nitrogen also alters CH_4 emissions through impacts on microbes and plants because nitrate inhibits methanotrophic activity by lowering redox potentials (Le Mer & Roger, 2001; Liu & Greaver, 2009), and affects wetland plant productivity and plant community composition, which influences CH_4 production, oxidation, and transport (Bubier et al., 2007). In addition, N inflow increases N_2O emissions by supplying more available N as materials for nitrifying and denitrifying bacteria (Dalal et al., 2003; Lohila et al., 2010).

Temperature is considered to be a major factor in regulating GHG emissions. An increase of N_2O and CO_2 emissions, but not CH_4 emissions were found with increasing temperature in wetlands soils under laboratory conditions (Schaufler et al., 2010). However, methanogenesis is more sensitive to temperature than respiration and photosynthesis (Inglett et al., 2012; Yvon-Durocher et al., 2014). Few studies have investigated the interaction of temperature, hydrology (Huang et al., 2016), and N availability (Stadmark & Leonardson, 2007).

Here, our objective was to investigate the likely ranges and drivers of GHG emissions in coastal wetlands of the Great Lakes region, USA (Figure S1), across their realistic ranges of hydrologic, temperature, and N inflow regimes (Table S1). Ecosystem models are ideally suited to this type of analysis and can help to synthesize our understanding, simulating consistent ranges and combinations of drivers not possible to achieve in field studies for such a large-scale region. We used MONDRIAN (Modes Of Nonlinear Dynamics, Resource Interactions, And Nutrient cycling), a process-based simulation model of wetland community-ecosystem processes (Currie et al., 2014; Martina et al., 2016). Knowing how processes interact in the model (Figure 1), we expected several key patterns to emerge. First, wetland N inflow should be positively related to C sequestration (negative NEE), through higher plant and litter production, when water levels remain high enough to maintain flooded litter and detrital pools in the model. Second, lower water levels that expose detrital pools to aerobic conditions should decrease C sequestration by increasing decay rates but should also decrease CH_4 and increase N_2O emissions due to aerobic conditions in upper soil. Third, greater water

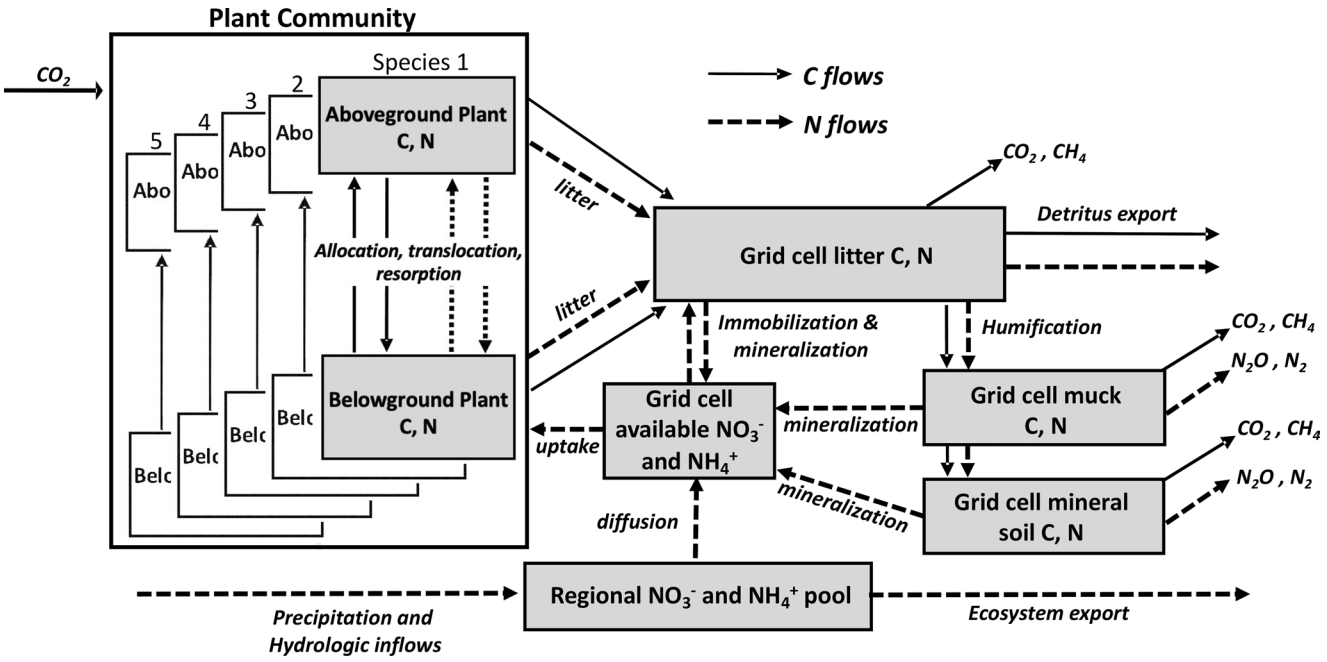

Figure 1. Carbon flows and nitrogen flows interacted in MONDRIAN, including biological and physical processes. The solid line represents C flows while the dashed line represents N flows.

residence time (for a given level of N inflow and assuming water levels maintain flooded conditions) should be related to more C sequestration through increased plant N uptake and productivity, but should also produce more N_2O emissions through greater nitrification and denitrification and more CH_4 emissions through greater C cycling. Finally, we expected the higher simulated temperature to produce less C sequestration in the model by increasing detrital decay rates and to produce more N_2O and CH_4 emissions through greater microbial activity. A key strength in using MONDRIAN was the ability to not only simulate the processes regulating individual GHG fluxes but also to compare their shifting contributions to SGWP across a range of realistic conditions in the Great Lakes region.

2. Methods

2.1. Overview of MONDRIAN Model

MONDRIAN is a process-based simulation model of wetlands that operates on a daily time step and spans multiple levels of ecological organization, including individual plant physiology, plant population growth and decline, plant community shifts through competition, and dynamics in ecosystem biogeochemistry including complete C and N cycles (Currie et al., 2014). Recent MONDRIAN versions integrate more detailed plant physiology and competition, including clonal branching and light competition (Goldberg et al., 2017; Martina et al., 2016). Nitrogen (N) cycling in MONDRIAN was also recently enhanced by adding nitrification and denitrification (Sharp et al., 2020). The model has previously been applied in Great Lakes coastal wetlands; however, the model processes are general enough that they could be used to study inland wetlands and wetlands in other regions.

Plant growth, population dynamics, and community composition shift in response to environmental drivers in MONDRIAN, including water level (which can fluctuate daily), water residence time, temperature, and N inflows. At the individual level, MONDRIAN simulates C and N uptake within each plant and neighboring plants compete for soil-available N and light within spatially explicit grid cells, leading to heterogeneous N availability. At the population level, plants reproduce clonally by creating daughter ramets using C and N reserves from connected parent rhizomes. At the ecosystem level (Figure 1), C and N enter the wetland through photosynthetic capture of C and hydrologic inflow of N that is assimilated in living tissue. C and N enter the litter pools after seasonal tissue senescence or from plant mortality. Decomposition of litter then

results in the mineralization of organic C and N. Rates of litter decomposition can be significantly slowed under low temperature and anaerobic conditions caused by high water level, defined in MONDRIAN as any portion of soil below a 5-day trailing average of water level (Reddy & DeLaune, 2008). Thus, flooding enhances C and N accretion in detritus while slowing the release of both C and N from detrital pools via mineralization. Previous studies using MONDRIAN provide greater detail on C and N cycling in the model, including controls on decomposition, decomposition feedbacks on N mineralization, plant growth and uptake of N, hydrology and anaerobic zonation and their effects on C and N cycling (Currie et al., 2014; Martina et al., 2016; Sharp et al., 2020).

For the present study, we enhanced MONDRIAN to include net emissions of GHGs CO_2, CH_4, and N_2O. As in previous applications of MONDRIAN, we conducted an ensemble of over 1,000 model simulations (described below) of a 52.5 × 52.5 cm^2 area consisting of 49 grid cells each 7.5 × 7.5 cm^2 in area. This area contains thousands of individual plants that reproduce and branch belowground spatially within a torus topology (Currie et al., 2014).

2.2. Net Ecosystem Exchange of CO_2

We drew on the existing complete ecosystem C balance in MONDRIAN to calculate the net ecosystem exchange (hereafter NEE) of CO_2-C as a model result. It is equal to the CO_2 emission from heterotrophic respiration minus the CO_2 sink in net photosynthesis, with a positive NEE defined as net emission and negative NEE defined as net C sequestration. The NEE calculation from our model results replicates what is measured as NEE of CO_2-C in field studies.

2.3. Methane Flux Simulation Sub-Model

Several process-based models have been developed to estimate CH_4 emissions across a range of ecosystems, including wetlands. Each has unique methods for dealing with wetland system complexity and CH_4 flux processes (Cao et al., 1996; Gerten et al., 2004; Oikawa et al., 2017; Riley et al., 2011; Sitch et al., 2003; Tian et al., 2010; Zhu et al., 2014). As all of these models did, we involved water level as an essential factor in defining anoxic and oxic soil zones where CH_4 is produced and oxidized, to modulate methane emissions.

We augmented MONDRIAN to include sophisticated CH_4 flux using a modified sub-model from Cao et al. (1996), which separately calculated CH_4 production and consumption in soil. Existing MONDRIAN processes first calculated total heterotrophic C respiration in each soil horizon based on model production and inputs of plant detritus together with user-specified detritus decay constants (separate decay constants for litter, muck, and mineral soil organic matter) modified by daily temperature and daily aerobic or anaerobic conditions in the model. The new sub-model then calculated the daily rate of CH_4-C production as a proportion, CH_4P, of total heterotrophic C respiration (C_{HR}) that undergoes methanogenesis to CH_4 (Equation 1).

$$\mathrm{CH4-C\ production} = \mathrm{CH_4P} * \mathrm{C_{HR}} \tag{1}$$

A user-specified parameter (CH_4P_0) specified the value of CH_4P under optimal conditions for methanogenesis, which was then scaled back on a daily basis for non-optimal temperature and soil water status (Equations 2–5).

$$\mathrm{CH_4P} = \mathrm{CH_4P_0} * f_{\mathrm{WLP}} * f_T \tag{2}$$

$$f_{\mathrm{WLP}} = 0.383 * e^{\left(0.096*100*\mathrm{WL}\right)} \tag{3}$$

$$\begin{cases} f_T = \dfrac{e^{(0.0693 * \mathrm{WT})}}{8} & (\mathrm{WT} > 0) \\ f_T = 0 & (\mathrm{WT} \le 0) \end{cases} \quad (4)$$

$$\begin{cases} \mathrm{WT} = 3.4 + 0.785 * T_{\mathrm{air}} & (\mathrm{TT}_{\mathrm{air}} > 0) \\ \mathrm{WT} = 3.5 & (T_{\mathrm{air}} \le 0) \end{cases} \quad (5)$$

In other wetland modeling studies, values of the proportion CH_4P_0 ranged from 0.1 to 0.3 (Riley et al., 2011; Wania et al., 2010; Zhu et al., 2014). We tested values of 0.1, 0.15, 0.2, 0.3, 0.4, and 0.47 in MONDRIAN during sub-model development using in-field data from five sites in North America (Minnesota, Ontario, Alaska, Michigan, and California). When $CH_4P_0 = 0.2$, we minimized squared error in testing our results against field measurements from the literature. We use $CH_4P_0 = 0.2$ in all model runs in this study.

In Equations 2–5, f_{WLP} is a function of water level position (cm), representing an index from 0 to 1 that lowers CH_4 production based on non-ideal conditions of aerobic related to water level. WL (cm) represents water level, which may be above or below the soil horizon. MONDRIAN calculates WL using a trailing average water level of 5 days to account for the delay in the switch from aerobic to anaerobic conditions (Sharp et al., 2020). The effect of temperature (°C) is f_T (Equation 4), where WT represents water temperature, which is calculated from air temperature (T_{air}) (Equation 5). An index f_T from 0 to 1 lowers CH_4 production based on water temperature with a maximum value of 1 at 30°C and a value of 0.12 at 0°C (Cao et al., 1996; Dunfield et al., 1993). If water temperature is 0 or below, CH_4 production is halted in the model by setting f_T to 0. Coefficients in equations came from Cao et al. (1996) and were calibrated into MONDRIAN.

MONDRIAN did not explicitly simulate fine-scale processes of CH_4 transport by diffusion, ebullition, and transport through plant tissues, which were implicitly included in the model scaling parameters for CH_4 production and oxidation. Oxidation of methane before emission from the wetland is accounted for as shown in Equation 6:

$$\text{Emission of } CH_4 - C = CH_4 - C \text{ production} * \left(1 - CH_4Ox\right) \quad (6)$$

In MONDRIAN, we used a value of $CH_4Ox = 0.43$ when muck is aerobic (Roslev & King, 1996) and $CH_4Ox = 0$ under anaerobic, inundated conditions (Equation 6). These oxidation rates (CH_4Ox) of CH_4 were user-defined inputs in MONDRIAN and could be changed by a model user to reflect conditions different from those in the current study.

2.4. N_2O Flux Simulation Sub-Model

Denitrification produces two species of gaseous N: N_2O and N_2. N_2O is a GHG with high radiative forcing while N_2 is inert. In wetlands, oxygen availability is an important factor in regulating N_2O production. Aerobic conditions enable nitrification (the production of NO_3^-), the primary reactant for N_2O production. Nitrate (NO_3^-) either flowing into a wetland or produced through nitrification then requires anaerobic conditions to be converted to N_2O. Oxygen availability also controls the N_2O-N yield (N_2O-N/(N_2O-N + N_2-N)) in denitrification N flux (Tiedje, 1988); hereafter N_2O yield. In MONDRIAN, total denitrification was calculated by NO_3^- availability, rate of heterotrophic CO_2 production, and anaerobic zone proportion (Sharp et al., 2020). For the present study, we augmented the existing sub-model of total denitrification to further calculate N_2O yield. We used water level and flooding days to represent oxygen ability and set N_2O yield to be 50% on the first day of flooding, 8% between 2 and 4 days of flooding, and 1% after 4 days of flooding (see justification below). We use daily water levels to represent aerobic and anaerobic conditions in the N_2O sub-model. All detrital pools (or proportions thereof), including above-and belowground litter, muck, and mineral soil organic matter (MSOM) pools lying below the level of the 5-day trailing average in water level are considered anaerobic.

N_2O yield is typically described in the literature as decreasing with increasing soil water content (Colbourn & Dowdell, 1984; Davidson, 1992; Rudaz et al., 1999), particularly when the soil water content exceeds 75% water-filled pore space (Davidson, 1992; Weier et al., 1993). High ratios of N_2O yield have also been observed

in the field and lab experiments on the first day of flooding events, relative to subsequent days because the transition from aerobic to anaerobic conditions increased the formation of N_2O (Ciarlo et al., 2007; Hansen et al., 2014; Lewicka-Szczebak et al., 2015). Experiments with 15N isotopes showed that N_2O yield decreased from 50% to below 5% after 4-day flooding (Hansen et al., 2014; Lewicka-Szczebak et al., 2015). Mean N_2O yield of 8.2% was measured in freshwater wetlands and flooded soils (Schlesinger, 2009), and mean N_2O yield of 0.9% in streams and rivers (Beaulieu et al., 2011). Average N_2O yield in soils under natural recovering vegetation is 49.2% (Schlesinger, 2009).

2.5. Model Parameterization and Simulations

In this study, we conducted sets of contrasting simulation model runs (one model run is a single 40-year simulation), that included 480 unique combinations of model drivers and parameters (six levels of water level scenarios, Figure S2; five levels of N inflow, four levels of water residence time, and four levels of temperature; Table S1). Each combination was replicated three times with stochastic differences both in initial plant distributions and spatial patterns of clonal reproduction and branching. In all model runs, our key dependent variables stabilized by 30–40 years, while continuing to show small fluctuation; thus for all analyses, the average of the last 5 years (years 36–40) of each model run was used.

We selected six water level scenarios to represent possible water levels found in coastal wetlands in Michigan (Figures S1 and S2). The six hydrologic regimes were as follows: (a) always anaerobic (constant water level 0.1 m above the MSOM surface); (b) always aerobic (water level constant at 0.1 m below the MSOM surface); (c) always aerobic (water level constant at 0.02 m below the MSOM); (d) sinusoidal fluctuation in the water level of −0.1 to 0.26 m about the MSOM surface with an annual hydroperiod (highest in July and lowest in January; NOAA Tides and Currents, 2020); (e) sinusoidal fluctuation in the water level of −0.1 to 0.26 m about the MSOM surface with an annual period together with a smaller, 5-day fluctuation superimposed; and (f) sinusoidal fluctuation in the water level of −0.26 to 0.1 m about the MSOM surface with an annual period together with a smaller, 5-day fluctuation superimposed.

We included five nitrogen inflow levels in this study (Table S1): 1, 5, 10, 15, and 20 g N m^{-2} yr^{-1}. Earlier modeling results (Martina et al., 2016) showed that *Phragmites* invasions, which dramatically change the ecosystem, failed at N inflow <4 g N m^{-2} yr^{-1} and a threshold for highly successful invasion usually occurred between 12 and 18 g N m^{-2} yr^{-1}. Our choices of N inflow levels span across the range of this threshold area, resulting in both successful and unsuccessful invasion.

There are few measurements of water residence time in Great Lakes coastal wetlands. Sierszen et al. (2012) used isotopes to measure the water residence time in coastal wetlands and found it to range from 0.16 to 46 days across their study sites. We estimated a wide range based on the variety of coastal wetlands in the region (Sharp et al., 2020), including 1, 10, 30, and 100 days (Table S1).

We set four annual-average temperature levels (10.2, 11.5, 13.5, and 14.5°C; Table S1) and allowed seasonal temperatures to vary around the specified annual average. 10.2°C was the average annual temperature in 1951 (GLISA, 2020) and 11.5°C represented the current temperature. Values of 13.5 and 14.5°C were estimated annual average temperatures in the Great Lakes by midcentury under low and high emissions scenarios (Hayhoe et al., 2010).

Climate change and warming are predicted to lengthen growing seasons in many parts of the world, including the Great Lakes region. Furthermore, temperature increases affect the growing season start and end dates unequally, resulting in the growing season start in the spring advancing by more days than the growing season end date is delayed in the fall (Linderholm, 2006). With 1°C increase in temperature the average annual growing season has advanced by 4–10.8 days in spring and has been extended by 1–7 days in autumn (Chmielewski & Rötzer, 2001; Ibáñez et al., 2010; Menzel & Fabian, 1999; Song et al., 2010; Wolfe et al., 2005; Zhou et al., 2001). Therefore, we represented growing season length in our simulations as a function of temperature. We set plant growing season changes for all four plant species in MONDRIAN with 7 days advance in spring and 4 days delay in autumn for each 1°C temperature increase.

Parameterized species used in this study included three native species (*Eleocharis palustris, Juncus balticus*, and *Schoenoplectus acutus*) and one invasive species (*Phragmites australis*) commonly occurring in Great

Lakes coastal wetlands (MONDRIAN has the potential to simulate five plant species; Figure 1). Native species were randomly distributed in the modeling area and given 14 years to become well established, while invasive (*Phragmites*) plants were introduced at random locations in year 15. While we do not expressly address plant invasion in the present study, previous work with MONDRIAN has shown that this produces a realistic range of plant communities over a range of N inflow levels (Currie et al., 2014; Martina et al., 2016; Sharp et al., 2020).

2.6. Calculation of SGWP and Statistical Analysis

SGWP is an advanced metric used to compare sustaining emissions of GHGs from ecosystems by standardizing their radiative effects in the atmosphere over a specific time horizon. Compared with the more widely used metric global warming potential (GWP), SGWP treats GHG emission as a persistent event instead of a one-time pulse, which is more realistic for the ecosystem fluxes (Neubauer & Megonigal, 2015). Here, we use $SGWP_{20}$ and $SGWP_{100}$ to denote 20-year and 100-year time horizons, respectively. SGWP is defined as the cumulative radiative forcing of each gas over the time period of interest divided by the cumulative radiative forcing of CO_2 over the same period, indicating how many kilograms of CO_2 must be sequestered to offset the emission of 1 kg of CH_4 and N_2O (Neubauer & Megonigal, 2015). Thus, SGWP values are reported as kg CO_2 equivalents (kg CO_2-eq). SGWP conversions for methane (CH_4) are 96 for $SGWP_{20}$ and 45 for $SGWP_{100}$; for N_2O the values are 250 for $SGWP_{20}$ and 270 for $SGWP_{100}$ (Neubauer & Megonigal, 2015). For results reported here, in addition to SGWP conversions to CO_2-eq, the fractions (44 g CO_2/12 g C), (16 g CH_4/12 g C), and (44 g N_2O/28 g N) were also used to convert from fluxes on a C or N mass basis in MONDRIAN model output (g CO_2-C m^{-2} yr^{-1}, g CH_4-C m^{-2} yr^{-1}, and g N_2O-N m^{-2} yr^{-1}) to the compound masses of the gases used in SGWP conversions. In addition, results reported here were converted to represent the net emission of each gas over 1 ha of wetland over one simulated year, thus reported as kg CO_2-eq ha^{-1} yr^{-1}. Our results include the $SGWP_{20}$ and $SGWP_{100}$ of each of the three GHGs considered individually as well as the net $SGWP_{20}$ and $SGWP_{100}$ (summed SGWP of CH_4, N_2O, and NEE of CO_2). We used ANOVA (factorial ANOVA, one-way ANOVA, Welch's ANOVA, depended on variances) and post hoc test (Tukey-HSD and Games-Howell) to assess differences in gas fluxes by water level scenario, water residence time, N inflow, and temperature using R version 3.6.3 (R Core Team, 2020). We checked the assumption of normality for each test but in some cases, the assumption was not meet. In these cases, we used a nonparametric aligned rank transform procedure which does not assume normality and got the consistent test results, meaning the parametric tests were robust to violations of the assumption of normality. For clarity, we present only the original parametric test results for these cases.

3. Results

We found the emission of CH_4, N_2O and net sequestration of C (negative NEE) increased with increasing water residence time and N inflow, primarily driven by increased plant productivity and N uptake, which in turn increased ecosystem C and N stocks. Our simulation results for the net $SGWP_{20}$ and $SGWP_{100}$ were dominated by the SGWP of CH_4. The SGWP of NEE was negative under most circumstances, meaning wetlands were net sinks of carbon in our simulations as wetland plants fix atmospheric CO_2 by photosynthesis and plant detrital pools accrete under inundated soil conditions. In our results, the SGWP of N_2O was negligible; although N_2O has high radiative forcing, the amount of N_2O emitted from wetlands in our simulations was very small. The net SGWP depended largely on how much the SGWP of CH_4 was offset by negative SGWP of NEE (CO_2). Water level scenarios also influenced GHG exchanges by modulating conditions between aerobic and anaerobic states. Generally, higher temperature promoted higher SGWP but due to the modest range of temperature increases we simulated, reflecting increases expected by the midcentury in this region, temperature effects were smaller than other drivers.

3.1. CH_4 Emission

CH_4 emissions ranged from near 0 to 73 g C m^{-2} yr^{-1} in our results. Teasing apart the main controls on CH_4 emissions in our results was challenging because there were many significant main effects and significant

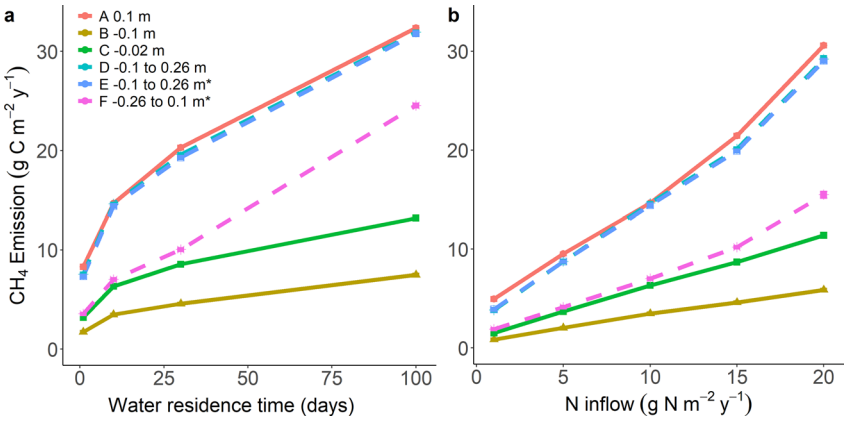

Figure 2. MONDRIAN model results for CH_4 emissions under current regional climate conditions (11.5°C annual mean temperature) as functions of water residence time (a) and wetland N inflow (b) in our simulations. Different lines refer to six different WL (water level) scenarios with constant (A–C) and seasonally fluctuating (D–F) water level. Asterisks (*) on legend indicate smaller 5-day fluctuations in water level superimposed on season fluctuations (Figure S2). Model results in panel (a) used an intermediate rate of N inflow of 10 g N m^{-2} yr^{-1}; model results in panel (b) used a low-intermediate water residence time of 10 days. Note that lines (D) and (E) are overlapping in both panels. Error bars represent standard errors among three replicate model runs; note that some error bars are within the size of the symbols and thus too small to be visible.

interactions among drivers ($p < 0.01$). However, among model runs, CH_4 emission increased the greatest and most consistent with increasing levels of N inflow and with longer water residence time (Figure 2).

Net primary productivity (NPP), a measure of ecosystem organic C, the primary substrate for methanogenesis and heterotrophic respiration, increased with increasing N inflow and water residence time as pools of available N were larger (reflected in plant uptake) thus facilitating increased plant growth (Figure 3). Higher N inflows provided more nitrogen in the ecosystem and under longer water residence time nitrogen could stay in the ecosystem longer instead of being flushed out, promoting more N uptake by plants. This was positively related to CH_4 production because greater NPP resulted in more litter production, which led to the accretion of detrital pools and higher levels of heterotrophic respiration. In MONDRIAN, CH_4 production is a function of heterotrophic respiration (Equations 1–6).

When controlling for N inflow, water residence time, and temperature, water level (WL) scenario (Figure S2) also had an important impact on the rates of CH_4 emission (Figure 2a). Notably, when water levels

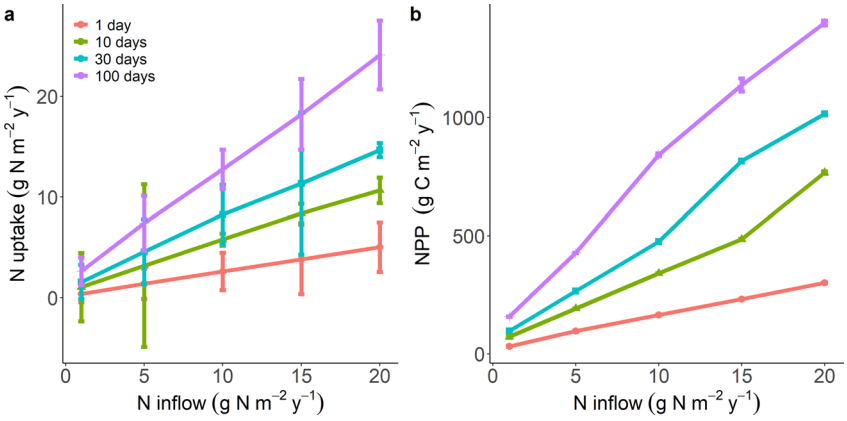

Figure 3. MONDRIAN model results for N uptake by plants (a) and NPP (b) as a function of wetland N inflow under scenarios under current regional climate conditions (11.5°C annual mean temperature) and water level scenario D (Figure S2). Different lines refer to different values of water residence time (days). Error bars represent standard errors among three replicate model runs; note that some error bars are within the size of the symbols and thus too small to be visible.

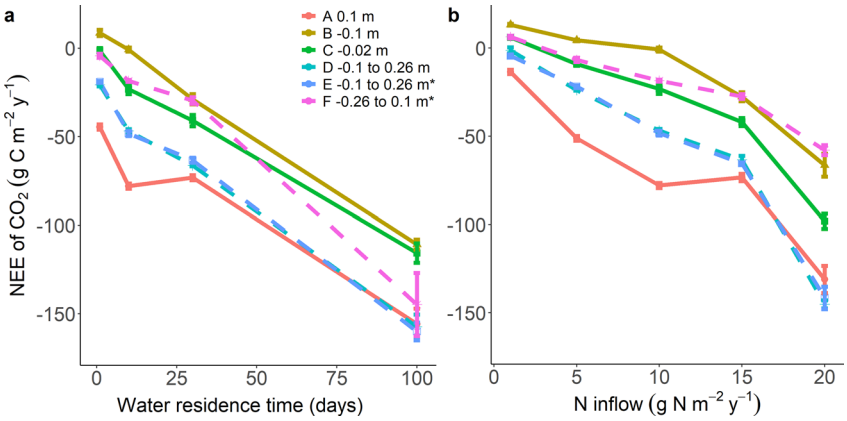

Figure 4. Net ecosystem exchange (NEE) of CO_2 as a function of wetland water residence time (a) and N inflow (b) under current regional climate conditions (11.5°C annual mean temperature). Negative values of NEE indicate a wetland sink of CO_2. Different lines refer to six different WL (water level) scenarios with constant (A–C) or seasonally fluctuating (D–F) water level (Figure S2). Asterisks on legend indicate smaller 5-day fluctuations superimposed on seasonally fluctuating water levels. Model results in panel (a) used an intermediate rate of N inflow of 10 g N m^{-2} yr^{-1}; model results in panel (b) used a low-intermediate water residence time of 10 days. Error bars represent standard errors among three replicate model runs; note that some error bars are within the size of the symbols and thus too small to be visible.

were constantly below zero (WL scenarios B and C) CH_4 emissions were lowest (0.313–26.9 g C m^{-2} yr^{-1}) and were significantly lower than other WL scenarios ($p < 0.01$). WL scenarios that had flooded periods, whether constant flooding at 0.1 m (WL scenario A) or seasonally fluctuating around the high level at 0.08 m (WL scenarios D and E) had the highest CH_4 emissions, but the three flooded WL scenarios (A, D, and E) were not significantly different from one another ($p = 0.99$). Fluctuation around an average low water level (WL scenario F, −0.08 m) with fewer days of the year flooded (132 days) had lower CH_4 emissions than fluctuating WL scenarios with high average water level (WL scenario D and E; 0.08 m) and more days of the years flooded (237 days; $p < 0.01$). Surprisingly, wetlands with a constant water level above the soil surface (0.1 m; WL scenario A) emitted less CH_4 than wetlands with fluctuating water around a positive mean (WL scenarios D and E) despite being flooded longer.

Although higher temperature stimulated higher CH_4 emissions, compared with N inflows and water residence time, the effects of our modest temperature changes (10.2–14.5°C) on CH_4 emissions were small. Only when temperature differences greater than 2°C were simulated values of CH_4 emissions significantly different ($p < 0.01$).

3.2. Net Ecosystem Exchange of CO_2

Similar to CH_4, NEE was strongly controlled by nitrogen inflow and water residence time (Figure 4). Because rates of photosynthesis and respiration largely determine rates of NEE, this component of SGWP is highly integrated with nitrogen availability. Under low nitrogen inflow (5 g N m^{-2} yr^{-1} or less) and low water residence time (10 days or less), negative NEE values (negative indicating net C sequestration) were relatively small in all simulations (ranging ca 16 to −60 g C m^{-2} yr^{-1}). But under high nitrogen inflow (20 g N m^{-2} yr^{-1}) and long water residence time (100 days), negative NEE values were relatively large, ranging from ca −150 to −270 g C m^{-2} yr^{-1}. When controlling for water residence time and temperature, greater levels of N inflow contributed to greater sequestration of C (negative NEE) in all WL scenarios (Figure 4).

Water level scenarios had a much smaller effect on NEE with longer flooding (WL scenarios A, D, and E) generally having more negative NEE by promoting more wetland C storage (Figure 4). Yearlong constant flooding (water scenario A) had more C storage than flooding for more than half a year (WL scenario D and E). WL scenarios D and E had more C storage than flooding for less days (WL scenario F) and water level scenarios with no flooding (B and C). Five-day fluctuation had little effect on NEE: NEE in WL scenario D and E were very similar because 5-day fluctuation did not change the total flooding days in 1 year. At

short to intermediate water residence time (1 day $p < 10^{-12}$, 10 days $p < 0.001$, 30 days $p < 0.01$), the NEE difference between water level scenarios was significant but not under the longest water residence time (100 days; $p = 0.34$).

Temperature differences had minor overall effects on NEE in our simulations. Higher temperatures simulated greater negative values of NEE, but the difference only became significant when the difference of temperature was greater than 2°C. Under the same N inflow, water residence time and WL scenario, the differences of NEE between 10.2 and 14.5°C were small, ranging from −16.6 to 68.8 g C m^{-2} yr^{-1} (median 11.1 g C m^{-2} yr^{-1}), compared with the overall range.

3.3. N_2O Emission

N_2O emissions increased with higher nitrogen inflows by increasing available N for denitrification and with longer water residence time by lowering wetland N export and increasing wetland N pools. However, unlike CH_4 emissions and NEE, 5-day fluctuations promoted more N_2O emissions. Additionally, N_2O had much lower emission rates (0–0.375 g N m^{-2} yr^{-1}) compared to CH_4 (0.313–73 g C m^{-2} yr^{-1}) and NEE (−270 to 16 g C m^{-2} yr^{-1}). In all water level scenarios, there were no N_2O emissions when water residence time was low (1 day) and N inflow was low (1 g N m^{-2} yr^{-1}). Under low nitrogen inflow level, as water residence time increased, N_2O emissions increased slowly (0–0.08 g N m^{-2} yr^{-1} from residence time of 1–100 days) while at high nitrogen inflow levels, N_2O emissions increased rapidly from 0 to 0.15 g N m^{-2} yr^{1} (data not shown). Greater levels of N inflow magnified the denitrification effects of longer water residence time.

Under the conditions of sufficient N inflow (≥10 g N m^{-2} yr^{-1}) and long enough residence time (100 days), the two fluctuating WL scenarios that included 5-day fluctuations (WL scenarios E and F) produced the greatest N_2O emissions. Fluctuation provided wetlands with more frequent transitions from aerobic to anaerobic conditions, which increased the N_2O yield from denitrification. Although 5-day fluctuations affected N_2O emission from denitrification compared to WL scenarios without 5-day fluctuations, this difference did not affect total N removed via denitrification (N_2 + N_2O). Despite different fluctuation patterns, water level scenarios D and E had very similar denitrification, nitrification, N uptake, and N retention, which also explained why WL scenario E did not show greater CH_4 emissions and higher negative value of NEE compared with WL scenario D. At constant −0.1 m water level (WL scenario B), there was zero N_2O emission because −0.1 m was below the "active zone" for denitrification that we set in MONDRIAN as a model parameter. Finally, N_2O emissions increased modestly with temperature but it was not significant ($p = 0.26$).

3.4. Sustained-Flux Global Warming Potential

In our simulations, SGWP of each GHG was controlled by the same drivers that controlled fluxes of each of the GHGs. For net SGWP (summed across the three GHGs), water residence time, N inflows, and water level (WL) scenarios were the most important drivers just as they were for the various GHGs that comprise the net SGWP. High N inflow and longer water residence time produced larger values of negative NEE but also greater CH_4 emissions. The SGWP of CH_4 emission consistently outweighed the negative SGWP of NEE, resulting in higher values of net $SGWP_{20}$ under higher N inflows and longer water residence times (data not shown). For the 100-year time horizon, this held true of all of the inundated water level scenarios (WL A, D, E, and F; Figure 5). However, in the low water level scenarios (WL B and C), net $SGWP_{100}$ decreased with high N inflow and long water residence time because the negative NEE effect outweighed the positive CH_4 emission (Figure 5); the SGWP of per unit CH_4 was much lower for the 100-year time horizon compared with the 20-year time horizon.

Across all model results, CH_4 was consistently the largest contributor for $SGWP_{20}$ (data not shown), NEE was the second-largest contributor, with negative SGWP. Although the SGWP for per unit mass of N_2O was highest among the three gases, its contribution to net SGWP was small compared with the other two gases because the amount of emitted N_2O was very small (shown in Figure 6 for $SGWP_{100}$). At the 100-year time horizon, across all N inflows, water residence times, and temperatures, CH_4 was the greatest contributor for SGWP in flooded water scenarios (A, D, E, and F), NEE was the second and N_2O was the least (e.g., Figure 6). In water scenario B (constant −0.1 m water level) where CH_4 emissions were smaller, NEE had a larger contribution and offset the SGWP of CH_4 and N_2O under high nitrogen inflows and long water

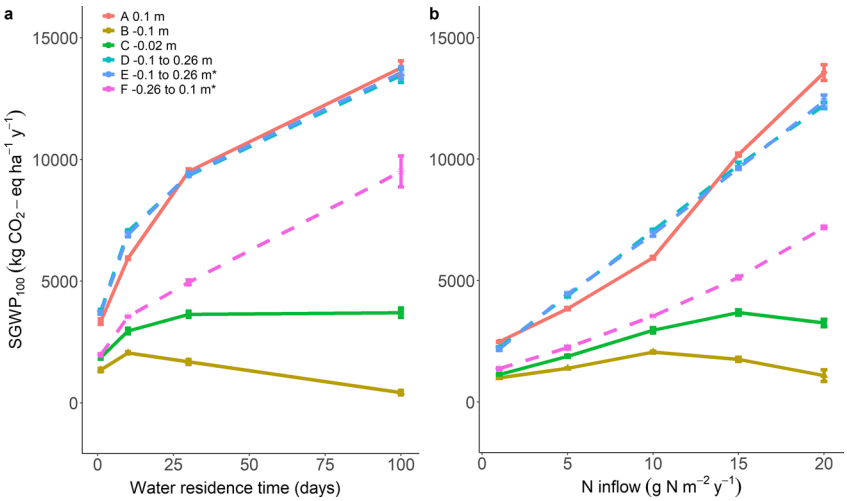

Figure 5. Model results for net global warming potential (SGWP) of three greenhouse gases as CO_2 equivalents (kg CO_2-eq ha^{-1} yr^{-1}) in the 100-year time horizon as functions of water residence time (a) and N inflow (b) under current regional climate conditions (11.5°C annual mean temperature). Different lines refer to six different WL (water level) scenarios with constant (A–C) or seasonally fluctuating (D–F) water level (Figure S2). Asterisks on legend indicate smaller 5-day fluctuations superimposed on seasonally fluctuating water levels. Model results in panel (a) used an intermediate rate of N inflow of 10 g N m^{-2} yr^{-1}; model results in panel (b) used a low-intermediate water residence time of 10 days. Error bars represent standard errors among three replicate model runs; note that some error bars are within the size of the symbols and thus too small to be visible.

residence time: in water scenario B, under water residence time 100 days, temperature 10.2°C and N inflow of 15 g N m^{-2} yr^{-1}, temperature 11.5°C and N inflow of 20 g N m^{-2} yr^{-1}, negative NEE counteracted SGWP of CH_4 and N_2O and made the net SGWP negative (−120 and −24 kg CO_2-eq ha^{-1} yr^{-1}). In water scenario C, NEE had similar contributions with CH_4 under long water residence time and high N inflow. Although the negative SGWP of NEE was still less than the positive SGWP of CH_4 and failed to counteract its influence, net SGWP in WL scenario C was much smaller than other scenarios.

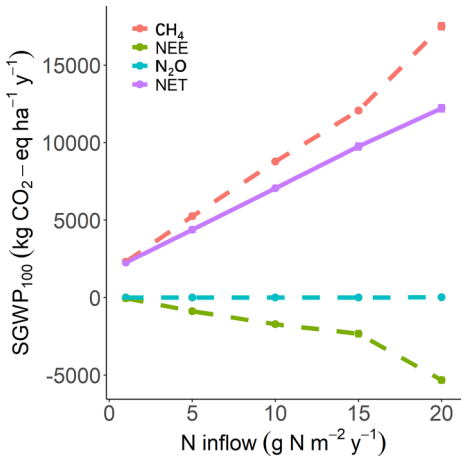

Figure 6. MONDRIAN model results for sustained-flux global warming potential (SGWP) of each GHG in the 100-year time horizon ($SGWP_{100}$) as functions of N inflow under current regional climate conditions (11.5°C annual mean temperature), water residence time 10 days and WL scenario D. Error bars represent standard errors among three replicate model runs; note that some error bars are within the size of the symbols and thus too small to be visible. NEE = net ecosystem exchange of CO_2; NET = net SGWP from three gases shown.

Similar to its component gases, net SGWP was also affected by WL scenarios. Flooding water level scenarios (WL scenarios A, and E, fluctuated from −0.1 to 0.26 m) had the highest net SGWP. Water scenarios B and C (constant negative water level) were significantly lower than others after controlling water residence time, nitrogen inflow, and temperature. Generally, net SGWP increased with temperature, but the effect size of temperature on net SGWP was small.

Scaling up our results, the net $SGWP_{20}$ of a 1-ha wetland ranged from 879 to 86,000 (kg CO_2-eq ha^{-1} yr^{-1}). The smallest value appeared in water level scenario C, when temperature was 10.2°C, water residence time was 1 day, and nitrogen inflow was 1 g N m^{-2} yr^{-1}. The highest $SGWP_{20}$ appeared in water scenario E, when temperature was 13.5 °C, water residence time was 100 days and nitrogen inflow was 20 g N m^{-2} yr^{-1}. $SGWP_{100}$ of 1-ha wetland ranged from −120 to 36,800 kg CO_2-eq ha^{-1} yr^{-1}. The smallest number appeared in water level scenario B, when temperature was 10.2°C, water residence time was 100 days, and nitrogen inflow was 15 g N m^{-2} yr^{-1}, producing C sequestration and negative NEE but without significant CH_4 emissions. The highest $SGWP_{100}$ appeared in water scenario E (more realistic flooding and water level fluctuation), when temperature was 14.5°C, water residence time was 100 days, and nitrogen inflow was 20 g N m^{-2} yr^{-1}. The high plant productivity and litter production (Figure 3) produced large accumulations of detritus, which together with flooded conditions drove high CH_4 emissions.

4. Discussion

In our simulations, Great Lakes coastal wetlands functioned as net sinks for CO_2 but net sources for CH_4 and N_2O. The net sustained-flux global warming potential (summed SGWP of CH_4, NEE, and N_2O) on 20-year and 100-year time horizons was always positive.

4.1. Comparison With Measured Data

CH_4 emission rates from wetlands measured in empirical studies have ranged from −11.4 to 13,870 g C m^{-2} yr^{-1} in different wetland types (Table 1). Our results, from near 0 to 73 g C m^{-2} yr^{-1}, fell within this range. Similarly, most of our simulated values of NEE fell within field-observed values. NEE in our results ranged from small positive values (representing emission of CO_2), up to 16 g C m^{-2} yr^{-1}, to much larger negative values (representing a net ecosystem sink for CO_2), up to ca −270 g C m^{-2} y^{-1}. Values observed in empirical studies have ranged from −30 to −2,200 g C m^{-2} yr^{-1} (Table 1). There was a small amount of estimated positive NEEs in our results that were out of the range of those empirical studies, which occurred with low water levels (including low constant water level scenarios B, C, and low seasonal fluctuated water level scenario F) and under low N inflow and low water residence time. This should be viewed as an outlier result that arose from using a wide range of model drivers in factorial combinations. We included low water level scenarios that allowed us to capture the full range of water levels coastal wetlands may experience, particularly as Great Lakes water levels fluctuate on interannual and decadal time scales. Under a below-zero water level, detrital pools that had accumulated under previously flooded conditions (represented by standardized initial conditions) would be out of equilibrium under low levels of NPP and would thus show net CO_2 emission from heterotrophic decomposition. The small positive NEE is not realistic for Great Lakes coastal wetlands over the long term, but it could potentially occur in the medium-term (years) in a wetland undergoing terrestrialization, where new conditions of NPP and litter production are not high enough to offset elevated decomposition in previously accumulated detrital pools. This is consistent with previous findings that wetlands can be both sources and sinks of carbon, depending on their age, operation, and the environmental boundary conditions such as location and climate (Kayranli et al., 2010).

Emissions of N_2O in our simulations ranged from 0 to 0.375 g N m^{-2} yr^{-1}. In field measurements in wetlands from the literature, estimated N_2O emissions ranged from 0.013 g N m^{-2} yr^{-1} to very high levels of 365 g N m^{-2} yr^{-1} (Table 1). However, values in the literature above 0.28 g N m^{-2} yr^{-1} occurred in constructed wetlands (Table 1), making our modeling results in good agreement with the range of N_2O observed in non-constructed wetlands across a range of studies.

In general, our simulated wetlands were large sinks of CO_2, small sources of N_2O, and modest sources of CH_4. These broad findings are consistent with previous studies on wetlands GHG emissions (Beringer et al., 2013; McNicol et al., 2017; Tan et al., 2020; Wang et al., 2016). But in contrast with some previous studies in which CO_2 was the dominant gas contributing to overall GWP (Beringer et al., 2013; Krauss & Whitbeck, 2012; Tan et al., 2020), CH_4 was the main contributor to net SGWP in our study. This is partly caused by the different conversion metrics of GWP used in studies, but some results are still in contrary even using the same conversion metric (Beringer et al., 2013; Tan et al., 2020). In empirical studies, the amount of CH_4 emitted from wetlands has been shown to predominantly relate to water level, temperature, and carbon availability (Christensen et al., 2003; Moore et al., 1998; O'Connor et al., 2010). In simulation, we set 0.2 as the value of CH_4P_0 (Equation 2) and assumed 43% of methane is oxidized before being emitted to the atmosphere when passing upward through aerobic surface soil (muck) in the model (Equation 6). The final CH_4 emitted (after CH_4 oxidation), as a percentage of heterotrophic respiration in our results ranged from 1% to 10% depending on WL scenarios (data not shown). In the MONDRIAN model, these could be adjusted according to environmental conditions through the value of the user parameters CH_4P_0 and CH_4Ox (Equation 2). CH_4 emission varies by wetland types and seasons but is positively correlated with net ecosystem production (NEP), with around 3% of NEP ultimately emitted as CH_4 at peak production period (Le Mer & Roger, 2001; Whiting & Chanton, 1993). Assume at the optimal condition, the left 97% NEP all comes to C sequestration, with CO_2-eq conversions 96 for $SGWP_{20}$ and 45 for $SGWP_{100}$, the contribution of CH_4 to net SGWP is always greater than CO_2 (96*0.03 > 1*0.97 for $SGWP_{20}$ and 45*0.03 > 1*0.97 for $SGWP_{100}$).

Table 1
CH_4 Emissions, Net Ecosystem Exchange (NEE) (as CO_2), and N_2O Emissions in Wetlands

Site	Time	CH_4 g C m^{-2} yr^{-1}	Methods	References
Sub-arctic mire, Sweden	June 16–September 1	1.31–237	Closed chamber technique	Ström and Christensen (2007)
Constructed wetland, Estonia, Finland, Norway, and Poland	Summer and winter season, 2001–2003	−11.7 to 13,900	Dark chamber	Søvik et al. (2006)
Freshwater marsh, China	November–March	1.58–4.38	Single column sampling-separation system equipped with flame ionization detector	Zhang et al. (2005)
Coastal saline wetlands, China	September 2012 to August 2013	−3.23 to 43.4	Closed static chamber	Xu et al. (2014)
Restored wetlands, Skjern Meadows, Denmark	2009–2011	8.25–12.8	Eddy Covariance Technique	Herbst et al. (2013)
Peatland, Minnesota, United States	2009–2011	11.8–24.9	Eddy Covariance Technique	Olson et al. (2013)
Current study		0.313–73		
Site	Time	NEE g C m^{-2} yr^{-1}	Methods	References
Peatland, Minnesota, United States	2009–2011	−21 to −39.5	Eddy covariance technique	Olson et al. (2013)
Restored wetlands, Skjern Meadows, Denmark	2009–2011	−195 to −983	Eddy covariance technique	Herbst et al. (2013)
Cattail marsh, Canada	May 9, 2005 to May 30, 2006	−264	Eddy covariance technique	Bonneville et al. (2008)
Sedge fen, Finland	2004–2005	−55.5	Eddy covariance technique	Aurela et al. (2007)
Sub-arctic mire, Sweden	June 16–September 1	−2,390 to −2,990	Closed chamber technique	Ström and Christensen (2007)
Bogs and mires, Finland		−15 to −35	Estimated C accumulation from dry mass of peat	Turunen et al. (2002)
Current study		−271 to 16		
Site	Time	N_2O g N m^{-2} yr^{-1}	Methods	References
Constructed wetland, Netherlands	April–September 2009	0.32–1.21	Estimated denitrification with nitrogen budget	de Klein and van der Werf (2014)
Natural wetlands, Sanjiang Plain, China	Early May to late September (2002–2005)	0.11 to 0.28	Static dark chamber and gas chromatography techniques	Song et al. (2009)
Freshwater marsh, Sanjiang plain, China	July 7–September 27, 2005	0.071	Gas chromatograph (Agilent 4890)	Yang et al. (2013)
Peatland, Ontario, Canada	2005	0.013	Data not report	Bubier et al. (2007)
Restored emergent freshwater marsh, California, United States	February 20, 2014 to February 20, 2015	0.062	Permanently deployed chambers	McNicol et al. (2017)
Constructed wetlands, Estonia, Finland, Norway, and Poland	Summer and winter season, 2001–2003	−0.77 to 365	Dark chamber	Søvik et al. (2006)
Current study		0–0.375		

Note. Negative values of NEE indicate a wetland C sink.

Land use, land cover, vegetation, nutrients, humidity, water table, salinity, soil pH, and temperature are considered to influence the GHG emissions (Al-Haj & Fulweiler, 2020; Oertel et al., 2016; Tan et al., 2020). The net SGWP of GHGs also varies by climate, wetland types, vegetation, and nutrients. Most field measurements only focused on one wetlands class and in one season yet exhibited the large range of calculated GWPs. In field studies of open-water wetlands with high ecosystem respiration, GWP of NEE did not offset GWP of CH_4 emission, producing an overall positive radiative forcing effect of 35,000 ± 3,000 kg CO_2-eq ha^{-1} yr^{-1} (McNicol et al., 2017) in 100-year time horizon, similar to the highest value in our results (Figure 6).

However, in natural wetlands with low water levels and low nitrogen loadings, negative SGWP of NEE offset the SGWP of CH_4 and N_2O, resulting in a negative net GWP (Beringer et al., 2013; Tan et al., 2020).

4.2. Drivers of Greenhouse Gas Emissions

4.2.1. N Inflow and Water Residence Time

Our results showed N inflow, water residence time and WL (water level) scenarios had significant effects on CH_4 emissions, sequestration of C (negative NEE), N_2O emissions, and net SGWP over both 20-year and 100-year time horizons. Previous studies have found that greater soil N content generally leads to higher soil respiration and to higher NEE, if carbon in detrital pools is not limiting (Niu et al., 2010; Peng et al., 2011). In coastal vegetation ecosystems, anthropogenic nitrogen loading is expected to increase CH_4 emissions (Al-Haj & Fulweiler, 2020). In MONDRIAN, higher levels of N inflow increased plant available N and longer water residence time decreased the flushing rate of N from the wetland downstream allowing greater wetland N retention (Sharp et al., 2020). Greater N stocks promoted greater plant NPP and greater sequestration of C (negative NEE; Martina et al., 2016). This stored organic C in detritus then provided the substrate for CH_4 production and emission. A benefit of modeling exercises like ours is that the precise mechanisms that gave rise to the model results can be clearly identified.

It was widely considered that N deposition would reduce SGWP owing to increased net CO_2 uptake (Wang et al., 2017). However, our study indicated that although high N inflow increased the sequestration of C, CH_4 emissions also increased with increasing net SGWP. Negative SGWP of NEE was unable to offset the N stimulated SGWP of CH_4 and N_2O emissions of all water scenarios in 20 years. In the 100-year time horizon, net SGWP in WL scenarios B and C (low constant water levels) decreased with high N inflow and water residence time. Negative SGWP of NEE offset the N stimulated SGWP of CH_4 and N_2O in this WL B. As Liu and Greaver (2009) showed, different ecosystems had different GHG responses with increasing N, such that N increased the GHG sink strength for forest ecosystems but agricultural ecosystems were sources for GHG emissions under intensive N application, with differences between forests and agricultural fields possibly being caused by different hydrology and nitrogen inputs.

4.2.2. Water Level Scenario

Our model results on constant water level scenarios are consistent with previous findings that high-water table increases CH_4 emissions (Blodau & Moore, 2003; MacDonald et al., 1998; Moore & Dalva, 1993; Yang et al., 2013). Water level scenarios constantly below zero (WL scenarios B and C) had lower CH_4 emissions than WL scenario A (constant above ground water level) because the aerobic soil condition decreased CH_4 production and increased oxidation. Five-day water level fluctuations in WL scenario E had limited effects on CH_4 emissions, relative to WL scenario D that omitted the 5-day fluctuation, because there was no difference in the annual number of flooded days and trailing average water level.

Water level scenarios also influenced NEE but to a lesser degree. We believe this is because in the lowest WL scenario (B, −0.1 m constant) plants become more productive due to the fast turnover of N, yet CO_2 mineralizes quickly. Although low water level encourages CO_2 emission, faster CO_2 uptake offset emissions, resulting in little difference in NEE between water level scenarios.

Because of the large reduction of CH_4 emissions caused by low water level, above-ground WL scenarios (including constant and seasonal fluctuating) had much higher net SGWP than below ground WL scenarios in 20 and 100 years. In a field experiment in Tibetan wetlands, lowering the water table 0.2 m reduced GWP from 337.3 to −480.1 g CO_2-eq m^{-2}, mostly because of decreased CH_4 emissions (Wang et al., 2017).

4.2.3. Temperature

Higher soil temperature leads to increased microbial metabolism, higher soil respiration rates, and greater emissions. Lu et al. (2017) found CO_2 was mainly regulated by annual temperature. CH_4 and N_2O fluxes also display strong and asynchronous seasonal dynamics (McNicol et al., 2017).

All of the GHG emissions we simulated are sensitive to temperature in MONDRIAN. However, we found that temperature differences and the associated differences in growing season length were less important than hydrology and nitrogen inflows in controlling GHG emissions. Temperature effects were small for all

three GHGs and net SGWP. In our simulations, the realistic range of temperature scenarios that we used had a much smaller impact on GHG emissions than the realistic, more widely ranging values of other drivers. As outlined above, our higher temperature scenarios did include longer plant growing seasons, allowing greater NPP and litter production. However, our simulations did not include a higher maximum net growth rate for plants. We believe this was the most parsimonious assumption given uncertainties about gross photosynthesis versus plant respiration together with uncertainties in complex, species-specific interactions between moisture and temperature effects on plant growth (Fang & Moncrieff, 2001).

4.3. Strength and Shortcoming of a Modeling Approach

Similar to most ecosystem models, MONDRIAN model gas fluxes driven by the biological process of plants and microorganisms, along with physical processes controlled by environment conditions (Figure 1; Grant et al., 2010; Riley et al., 2011; Wania et al., 2010). However, there are only a few ecosystem models that simultaneously model three GHGs; most ecosystem models only focus on CH_4 and CO_2 or N_2O. We used MONDRIAN to simulate three GHGs under variable environmental conditions, which helps to illustrate the linkage and interaction between plant ecology, hydrology, N cycling, and C cycling.

In contrast with field measurements and other ecosystem models that only look at one or two environment factors or GHGs at one time, MONDRIAN has the strength to perform large factorial sets of runs to investigate the role of multiple environmental factors on the emission of three GHGs. This provided us enough data to explore which interactions among drivers and environmental conditions may be the most important in determining GHG emissions and net SGWP.

At the same time, because the strength of a model like MONDRIAN is that it integrates multiple processes and drivers in a full community-ecosystem model, a limitation is that it does not model individual biogeochemical processes with as much detail as some other models that have a different focus (Li et al., 2000; Riley et al., 2011). We did not include some environmental conditions such as pH and E_h into sub-models for GHG emissions because of the variability in the literature on how pH and E_h influence GHG emissions. This may increase uncertainty in our estimates of GHG emissions: CH_4 and N_2O are known to be sensitive to pH and E_h (Weslien et al., 2009), which may influence net SGWP. E_h and pH can vary among wetlands likely causing spatial heterogeneity of GHG emissions and SGWP.

Methane transport from anoxic sediments to the atmosphere occurs by three main pathways: diffusion, ebullition, and plant vasculature. These three pathways differentially influence the rate of CH_4 emissions (Chanton, 2005; McNicol et al., 2017). In MONDRIAN, we did not explicitly simulate fine-scale processes of gas transport by diffusion, ebullition, and transport through plant tissues. However, in some other current models that simulate CH_4 in greater detail these pathways are considered (Riley et al., 2011; Wania et al., 2010; Zhu et al., 2014). We made the gross assumption that 43% (Roslev & King, 1996) of CH_4 production was oxidized before emission, without specifying details of CH_4 transport processes or how those processes might shift with water level, plant species, or other factors. This assumption may introduce uncertainties to our estimated net SGWP. However, even though direct plant effects (e.g., transport through plant vasculature) are not in MONDRIAN explicitly, they are included implicitly because we compared our modeled methane net emissions against studies of emissions that did included the influence of plants (Table 1). In MONDRIAN, plants have indirect effects on methane emissions by influencing the quantity and quality of organic matter available for biogeochemical processes in detritus (decomposition, methanogenesis, and denitrification).

Nitrate and denitrification products NO and N_2O can lower redox potentials (Le Mer & Roger, 2001; Liu & Greaver, 2009) and inhibit CH_4 production, depending on the type of methanogenic bacterium present and the concentration of each N-compound (Klüber & Conrad, 1998). Although MONDRIAN links C cycling and N cycling, the competition between methanogenesis and denitrification is currently omitted in the model. We assumed that denitrification and methanogenesis can happen simultaneously, which could overestimate CH_4 emissions under conditions where nitrate is readily available. Future model enhancements could address this interaction and could also include the process of N-mediated anaerobic oxidation of CH_4 as a potentially important N and methane interaction. However, as described above, our modeled emission rates for CH_4 and N_2O are within the range of field obtained rates. This suggests that the model

simplifications in MONDRIAN allow simulation of net GHG fluxes in the correct range obtained in field studies, although the differential fluxes under different drivers and their interactions need further study both in models and in field studies.

Future research could include model enhancements to provide increased process-level detail or new field studies to test and further explore the interactions identified here. Increased process-level details could include the potential effects of plant species changes in mediating net CH_4 emissions, indicating different pathways of CH_4 and oxygen movement through wetlands in the controls over oxygen diffusion, depletion, and the time scale of fluctuations between aerobic and anaerobic conditions in detrital pools in different vertical layers as wetland water level rises and falls. Greater details on net N_2O production through nitrification could be modeled, including N_2O production through nitrification. Although in our study, temperature differences played a relatively minor role on GHG emissions, improved field studies of temperature sensitivity and heterogeneity would help to test this model result. Finally, field studies addressing the interaction of N inflows, water residence time, and net GHG emissions at appropriately large scales (meters to hundreds of meters in the field) are needed to test the complex interactions revealed by our modeling study.

5. Conclusion

In our simulations, Great Lakes coastal wetlands exhibited net sinks for CO_2 but net sources for CH_4 and N_2O and had positive net SGWP under most conditions, which suggests Great Lakes coastal wetlands could be sources of global warming under the realistic ranges of conditions and drivers we analyzed. Among the three GHGs we studied, CH_4 made the dominant contribution to net SGWP in our results and thus deserves more attention in future research. Water residence time, N inflow, and water level scenarios were most essential to three GHGs and net SGWP because they controlled N uptake by plants and plant productivity, which determined the amount of C that accumulated in detrital pools, leading to heterotrophic respiration that including CH_4 production. Greater N uptake related to positive ecosystem C storage but at the same time, provided more substrate for CH_4 production. Thus, the balance between CH_4 emission and C sequestration was shown to be a key SGWP tradeoff in wetlands we simulated. Temperature was the least important driver in our results, due in part to the limited temperature range we studied. However, our understanding of how temperature influenced GHG emissions involves simplifications and contains uncertainty. Field measurements and experiments under wide ranges of conditions and drivers are needed to provide the empirical basis for improving future integrative process models to represent these interactions with greater confidence.

Data Availability Statement

The MONDRIAN model (V4.3) source code is available through an open-source license, together with default versions of all input files and a detailed user guide at this website: http://williamcurrie.net/downloads/. A data set containing all of the input files, drivers, model results, and metadata from the analysis report here is freely available open-access through the University of Michigan Deep Blue permanent repository, DOI: https://doi.org/10.7302/2d96-ad40.

Acknowledgments
This study was funded, in part, by the School for Environment and Sustainability at the University of Michigan and in part by the National Aeronautics and Space Administration (NASA) IDS program, grant #80NSSC17K0262. The authors thank Laura Bourgeau-Chavez and Jeremy Graham from the Michigan Technological University for creation of the Great Lakes coastal wetlands map.

References

Al-Haj, A. N., & Fulweiler, R. W. (2020). A synthesis of methane emissions from shallow vegetated coastal ecosystems. *Global Change Biology*, *26*(5), 2988–3005. https://doi.org/10.1111/gcb.15046

Aurela, M., Riutta, T., Laurila, T., Tuovinen, J. P., Vesala, T., Tuittila, E. S., et al. (2007). CO_2 exchange of a sedge fen in southern Finland—The impact of a drought period. *Tellus B: Chemical and Physical Meteorology*, *59*(5), 826–837. https://doi.org/10.1111/j.1600-0889.2007.00309.x

Beaulieu, J. J., Tank, J. L., Hamilton, S. K., Wollheim, W. M., Hall, R. O., Mulholland, P. J., et al. (2011). Nitrous oxide emission from denitrification in stream and river networks. *Proceedings of the National Academy of Sciences of the United States of America*, *108*(1), 214–219. https://doi.org/10.1073/pnas.1011464108

Beringer, J., Livesley, S. J., Randle, J., & Hutley, L. B. (2013). Carbon dioxide fluxes dominate the greenhouse gas exchanges of a seasonal wetland in the wet–dry tropics of northern Australia. *Agricultural and Forest Meteorology*, *182*, 239–247. https://doi.org/10.1016/j.agrformet.2013.06.008

Blodau, C., Basiliko, N., & Moore, T. R. (2004). Carbon turnover in peatland mesocosms exposed to different water table levels. *Biogeochemistry*, *67*(3), 331–351. https://doi.org/10.1023/B:BIOG.0000015788.30164.e2

Blodau, C., & Moore, T. R. (2003). Experimental response of peatland carbon dynamics to a water table fluctuation. *Aquatic Sciences*, *65*(1), 47–62. https://doi.org/10.1007/s000270300004

Bonneville, M. C., Strachan, I. B., Humphreys, E. R., & Roulet, N. T. (2008). Net ecosystem CO_2 exchange in a temperate cattail marsh in relation to biophysical properties. *Agricultural and Forest Meteorology*, *148*(1), 69–81. https://doi.org/10.1016/j.agrformet.2007.09.004

Bridgham, S. D., Cadillo-Quiroz, H., Keller, J. K., & Zhuang, Q. (2013). Methane emissions from wetlands: Biogeochemical, microbial, and modeling perspectives from local to global scales. *Global Change Biology*, *19*(5), 1325–1346. https://doi.org/10.1111/gcb.12131

Bubier, J. L., Moore, T. R., & Bledzki, L. A. (2007). Effects of nutrient addition on vegetation and carbon cycling in an ombrotrophic bog. *Global Change Biology*, *13*(6), 1168–1186. https://doi.org/10.1111/j.1365-2486.2007.01346.x

Cao, M., Marshall, S., & Gregson, K. (1996). Global carbon exchange and methane emissions from natural wetlands: Application of a process-based model. *Journal of Geophysical Research*, *101*(D9), 14399–14414. https://doi.org/10.1029/96JD00219

Chanton, J. P. (2005). The effect of gas transport on the isotope signature of methane in wetlands. *Organic Geochemistry*, *36*(5), 753–768. https://doi.org/10.1016/j.orggeochem.2004.10.007

Chimner, R. A., & Cooper, D. J. (2003). Influence of water table levels on CO_2 emissions in a Colorado subalpine fen: An in-situ microcosm study. *Soil Biology and Biochemistry*, *35*(3), 345–351. https://doi.org/10.1016/S0038-0717(02)00284-5

Chmielewski, F. M., & Rötzer, T. (2001). Response of tree phenology to climate change across Europe. *Agricultural and Forest Meteorology*, *108*(2), 101–112. https://doi.org/10.1016/S0168-1923(01)00233-7

Christensen, T. R., Ekberg, A., Ström, L., Mastepanov, M., Panikov, N., Öquist, M., et al. (2003). Factors controlling large scale variations in methane emissions from wetlands. *Geophysical Research Letters*, *30*(7). 1414. https://doi.org/10.1029/2002GL016848

Ciarlo, E., Conti, M., Bartoloni, N., & Rubio, G. (2007). The effect of moisture on nitrous oxide emissions from soil and the $N_2O/(N_2O+N_2)$ ratio under laboratory conditions. *Biology and Fertility of Soils*, *43*(6), 675–681. https://doi.org/10.1007/s00374-006-0147-9

Colbourn, P., & Dowdell, R. J. (1984). Denitrification in field soils. *Plant and Soil*, *76*(1–3), 213–226. https://doi.org/10.1007/BF02205581

Currie, W. S., Goldberg, D. E., Martina, J., Wildova, R., Farrer, E., & Elgersma, K. J. (2014). Emergence of nutrient-cycling feedbacks related to plant size and invasion success in a wetland community–ecosystem model. *Ecological Modelling*, *282*, 69–82. https://doi.org/10.1016/j.ecolmodel.2014.01.010

Dalal, R. C., Wang, W., Robertson, G. P., & Parton, W. J. (2003). Nitrous oxide emission from Australian agricultural lands and mitigation options: A review. *Soil Research*, *41*(2), 165–195. https://doi.org/10.1071/SR02064

Davidson, E. A. (1992). Sources of nitric oxide and nitrous oxide following wetting of dry soil. *Soil Science Society of America Journal*, *56*(1), 95–102. https://doi.org/10.2136/sssaj1992.03615995005600010015x

de Klein, J. J., & van der Werf, A. K. (2014). Balancing carbon sequestration and GHG emissions in a constructed wetland. *Ecological Engineering*, *66*, 36–42. https://doi.org/10.1016/j.ecoleng.2013.04.060

Dinsmore, K. J., Skiba, U. M., Billett, M. F., & Rees, R. M. (2009). Effect of water table on greenhouse gas emissions from peatland mesocosms. *Plant and Soil*, *318*(1–2), 229–242. https://doi.org/10.1007/s11104-008-9832-9

Dunfield, P., Dumont, R., Moore, T. R., & Moore, T. (1993). Methane production and consumption in temperate and subarctic peat soils: Response to temperature and pH. *Soil Biology and Biochemistry*, *25*(3), 321–326. https://doi.org/10.1016/0038-0717(93)90130-4

Fang, C., & Moncrieff, J. B. (2001). The dependence of soil CO_2 efflux on temperature. *Soil Biology and Biochemistry*, *33*(2), 155–165. https://doi.org/10.1016/S0038-0717(00)00125-5

Forster, P., Ramaswamy, V., Artaxo, P., Berntsen, T., Betts, R., Fahey, D. W., et al. (2007). Changes in atmospheric constituents and in radiative forcing. In *Climate Change 2007: The physical science basis*.

Gerten, D., Schaphoff, S., Haberlandt, U., Lucht, W., & Sitch, S. (2004). Terrestrial vegetation and water balance—Hydrological evaluation of a dynamic global vegetation model. *Journal of Hydrology*, *286*(1–4), 249–270. https://doi.org/10.1016/j.jhydrol.2003.09.029

GLISA. (2020). *Climate change in the Great Lakes region references*. Retrieved from http://glisa.umich.edu/gl-climate-factsheet-refs

Goldberg, D. E., Martina, J. P., Elgersma, K. J., & Currie, W. S. (2017). Plant size and competitive dynamics along nutrient gradients. *The American Naturalist*, *190*(2), 229–243. https://doi.org/10.1086/692438

Grant, R. F., Black, T. A., Jassal, R. S., & Bruemmer, C. (2010). Changes in net ecosystem productivity and greenhouse gas exchange with fertilization of Douglas fir: Mathematical modeling in ecosys. *Journal of Geophysical Research: Biogeosciences*, *115*(G4). G04009. https://doi.org/10.1029/2009JG001094

Hansen, M., Clough, T. J., & Elberling, B. (2014). Flooding-induced N_2O emission bursts controlled by pH and nitrate in agricultural soils. *Soil Biology and Biochemistry*, *69*, 17–24. https://doi.org/10.1016/j.soilbio.2013.10.031

Hayhoe, K., VanDorn, J., Croley, T., II, Schlegal, N., & Wuebbles, D. (2010). Regional climate change projections for Chicago and the US Great Lakes. *Journal of Great Lakes Research*, *36*, 7–21. https://doi.org/10.1016/j.jglr.2010.03.012

Herbst, M., Friborg, T., Schelde, K., Jensen, R., Ringgaard, R., Thomsen, A. G., et al. (2013). Climate and site management as driving factors for the atmospheric greenhouse gas exchange of a restored wetland. *Biogeosciences*, *10*, 39–52. https://doi.org/10.5194/bg-10-39-2013

Huang, S., Sun, Y., Yu, X., & Zhang, W. (2016). Interactive effects of temperature and moisture on CO_2 and CH_4 production in a paddy soil under long-term different fertilization regimes. *Biology and Fertility of Soils*, *52*(3), 285–294. https://doi.org/10.1007/s00374-015-1075-3

Ibáñez, I., Primack, R. B., Miller-Rushing, A. J., Ellwood, E., Higuchi, H., Lee, S. D., et al. (2010). Forecasting phenology under global warming. *Philosophical Transactions of the Royal Society B: Biological Sciences*, *365*(1555), 3247–3260. https://doi.org/10.1098/rstb.2010.0120

Inglett, K. S., Inglett, P. W., Reddy, K. R., & Osborne, T. Z. (2012). Temperature sensitivity of greenhouse gas production in wetland soils of different vegetation. *Biogeochemistry*, *108*(1–3), 77–90. https://doi.org/10.1007/s10533-011-9573-3

IPCC. (2013). Climate change 2013: The physical science basis. In T. F. Stocker, D. Qin, G.-K. Plattner, M. Tignor, S. K. Allen, J. Boschung, et al. (Eds.), *Contribution of working group I to the fifth assessment report of the Intergovernmental Panel on Climate Change* (p. 714). Cambridge University Press.

Kayranli, B., Scholz, M., Mustafa, A., & Hedmark, Å. (2010). Carbon storage and fluxes within freshwater wetlands: A critical review. *Wetlands*, *30*(1), 111–124. https://doi.org/10.1007/s13157-009-0003-4

Kirschke, S., Bousquet, P., Ciais, P., Saunois, M., Canadell, J. G., Dlugokencky, E. J., et al. (2013). Three decades of global methane sources and sinks. *Nature Geoscience*, *6*(10), 813–823. https://doi.org/10.1038/ngeo1955

Klüber, H. D., & Conrad, R. (1998). Inhibitory effects of nitrate, nitrite, NO and N_2O on methanogenesis by *Methanosarcina barkeri* and *Methanobacterium bryantii*. *FEMS Microbiology Ecology*, *25*(4), 331–339. https://doi.org/10.1111/j.1574-6941.1998.tb00484.x

Krauss, K. W., & Whitbeck, J. L. (2012). Soil greenhouse gas fluxes during wetland forest retreat along the lower Savannah River, Georgia (USA). *Wetlands*, *32*(1), 73–81. https://doi.org/10.1007/s13157-011-0246-8

LeBauer, D. S., & Treseder, K. K. (2008). Nitrogen limitation of net primary productivity in terrestrial ecosystems is globally distributed. *Ecology*, *89*(2), 371–379. https://doi.org/10.1890/06-2057.1

Le Mer, J., & Roger, P. (2001). Production, oxidation, emission and consumption of methane by soils: A review. *European Journal of Soil Biology*, *37*(1), 25–50. https://doi.org/10.1016/S1164-5563(01)01067-6

Lewicka-Szczebak, D., Well, R., Bol, R., Gregory, A. S., Matthews, G. P., Misselbrook, T., et al. (2015). Isotope fractionation factors controlling isotopic signatures of soil-emitted N_2O produced by denitrification processes of various rates. *Rapid Communications in Mass Spectrometry*, *29*(3), 269–282. https://doi.org/10.1002/rcm.7102

Li, C., Aber, J., Stange, F., Butterbach-Bahl, K., & Papen, H. (2000). A process-oriented model of N_2O and NO emissions from forest soils: 1. Model development. *Journal of Geophysical Research*, *105*(D4), 4369–4384. https://doi.org/10.1029/1999JD900949

Linderholm, H. W. (2006). Growing season changes in the last century. *Agricultural and Forest Meteorology*, *137*(1–2), 1–14. https://doi.org/10.1016/j.agrformet.2006.03.006

Liu, L., & Greaver, T. L. (2009). A review of nitrogen enrichment effects on three biogenic GHGs: The CO_2 sink may be largely offset by stimulated N_2O and CH_4 emission. *Ecology Letters*, *12*(10), 1103–1117. https://doi.org/10.1111/j.1461-0248.2009.01351.x

Lohila, A., Aurela, M., Hatakka, J., Pihlatie, M., Minkkinen, K., Penttilä, T., & Laurila, T. (2010). Responses of N_2O fluxes to temperature, water table and N deposition in a northern boreal fen. *European Journal of Soil Science*, *61*(5), 651–661. https://doi.org/10.1111/j.1365-2389.2010.01265.x

Lu, W., Xiao, J., Liu, F., Zhang, Y., Liu, C. A., & Lin, G. (2017). Contrasting ecosystem CO_2 fluxes of inland and coastal wetlands: A meta-analysis of eddy covariance data. *Global Change Biology*, *23*(3), 1180–1198. https://doi.org/10.1111/gcb.13424

MacDonald, J. A., Fowler, D., Hargreaves, K. J., Skiba, U., Leith, I. D., & Murray, M. B. (1998). Methane emission rates from a northern wetland; Response to temperature, water table and transport. *Atmospheric Environment*, *32*(19), 3219–3227. https://doi.org/10.1016/S1352-2310(97)00464-0

Martina, J. P., Currie, W. S., Goldberg, D. E., & Elgersma, K. J. (2016). Nitrogen loading leads to increased carbon accretion in both invaded and uninvaded coastal wetlands. *Ecosphere*, *7*(9), e01459. https://doi.org/10.1002/ecs2.1459

McNicol, G., Sturtevant, C. S., Knox, S. H., Dronova, I., Baldocchi, D. D., & Silver, W. L. (2017). Effects of seasonality, transport pathway, and spatial structure on greenhouse gas fluxes in a restored wetland. *Global Change Biology*, *23*(7), 2768–2782. https://doi.org/10.1111/gcb.13580

Menzel, A., & Fabian, P. (1999). Growing season extended in Europe. *Nature*, *397*(6721), 659. https://doi.org/10.1038/17709

Mitsch, W. J., & Gosselink, J. G. (2007). *Wetlands* (4th ed.). John Wiley.

Mitsch, W. J., & Gosselink, J. G. (2015). Wetlands of the world. In W. J. Mitsch (Ed.), *Wetlands* (pp. 45–110). John Wiley & Sons.

Moore, T. R., & Dalva, M. (1993). The influence of temperature and water table position on carbon dioxide and methane emissions from laboratory columns of peatland soils. *Journal of Soil Science*, *44*(4), 651–664. https://doi.org/10.1111/j.1365-2389.1993.tb02330.x

Moore, T. R., Roulet, N. T., & Waddington, J. M. (1998). Uncertainty in predicting the effect of climatic change on the carbon cycling of Canadian peatlands. *Climatic Change*, *40*(2), 229–245. https://doi.org/10.1023/A:1005408719297

Neubauer, S. C., & Megonigal, J. P. (2015). Moving beyond global warming potentials to quantify the climatic role of ecosystems. *Ecosystems*, *18*(6), 1000–1013. https://doi.org/10.1007/s10021-015-9879-4

Niu, S., Wu, M., Han, Y. I., Xia, J., Zhang, Z. H. E., Yang, H., & Wan, S. (2010). Nitrogen effects on net ecosystem carbon exchange in a temperate steppe. *Global Change Biology*, *16*(1), 144–155. https://doi.org/10.1111/j.1365-2486.2009.01894.x

NOAA Tides and Currents. (2020). Retrieved from https://tidesandcurrents.noaa.gov/waterlevels.html?id=9099018&bdate=20100101&edate=20200101&units=metric&timezone=LST/LDT&interval=m

Nuansawan, N., Boonnorat, J., Chiemchaisri, W., & Chiemchaisri, C. (2016). Effect of hydraulic retention time and sludge recirculation on greenhouse gas emission and related microbial communities in two-stage membrane bioreactor treating solid waste leachate. *Bioresource Technology*, *210*, 35–42. https://doi.org/10.1016/j.biortech.2016.01.109

O'Connor, F. M., Boucher, O., Gedney, N., Jones, C. D., Folberth, G. A., Coppell, R., et al. (2010). Possible role of wetlands, permafrost, and methane hydrates in the methane cycle under future climate change: A review. *Reviews of Geophysics*, *48*(4). RG4005. https://doi.org/10.1029/2010RG000326

Oertel, C., Matschullat, J., Zurba, K., Zimmermann, F., & Erasmi, S. (2016). Greenhouse gas emissions from soils—A review. *Geochemistry*, *76*(3), 327–352. https://doi.org/10.1016/j.chemer.2016.04.002

Oikawa, P. Y., Jenerette, G. D., Knox, S. H., Sturtevant, C., Verfaillie, J., Dronova, I., et al. (2017). Evaluation of a hierarchy of models reveals importance of substrate limitation for predicting carbon dioxide and methane exchange in restored wetlands. *Journal of Geophysical Research: Biogeosciences*, *122*(1), 145–167. https://doi.org/10.1002/2016JG003438

Olson, D. M., Griffis, T. J., Noormets, A., Kolka, R., & Chen, J. (2013). Interannual, seasonal, and retrospective analysis of the methane and carbon dioxide budgets of a temperate peatland. *Journal of Geophysical Research: Biogeosciences*, *118*(1), 226–238. https://doi.org/10.1002/jgrg.20031

Peng, Q., Dong, Y., Qi, Y., Xiao, S., He, Y., & Ma, T. (2011). Effects of nitrogen fertilization on soil respiration in temperate grassland in Inner Mongolia, China. *Environmental Earth Sciences*, *62*(6), 1163–1171. https://doi.org/10.1007/s12665-010-0605-4

R Core Team. (2020). *R: A language and environment for statistical computing*. R Foundation for Statistical Computing. Retrieved from https://www.R-project.org/

Reddy, K. R., & DeLaune, R. D. (2008). *Biogeochemistry of wetlands: Science and applications*. CRC Press. https://doi.org/10.1201/9780203491454

Riley, W. J., Subin, Z. M., Lawrence, D. M., Swenson, S. C., Torn, M. S., Meng, L., et al. (2011). Barriers to predicting changes in global terrestrial methane fluxes: Analyses using CLM4Me, a methane biogeochemistry model integrated in CESM. *Biogeosciences*, *8*(7), 1925–1953. https://doi.org/10.5194/bg-8-1925-2011

Roslev, P., & King, G. M. (1996). Regulation of methane oxidation in a freshwater wetland by water table changes and anoxia. *FEMS Microbiology Ecology*, *19*(2), 105–115. https://doi.org/10.1016/0168-6496(95)00084-4

Rudaz, A. O., Wälti, E., Kyburz, G., Lehmann, P., & Fuhrer, J. (1999). Temporal variation in N_2O and N_2 fluxes from a permanent pasture in Switzerland in relation to management, soil water content and soil temperature. *Agriculture, Ecosystems & Environment*, *73*(1), 83–91. https://doi.org/10.1016/S0167-8809(99)00005-5

Saunois, M., Stavert, A. R., Poulter, B., Bousquet, P., Canadell, J. G., Jackson, R. B., et al. (2020). The global methane budget 2000–2017. *Earth System Science Data*, *12*(3), 1561–1623. https://doi.org/10.5194/essd-12-1561-2020

Schaufler, G., Kitzler, B., Schindlbacher, A., Skiba, U., Sutton, M. A., & Zechmeister-Boltenstern, S. (2010). Greenhouse gas emissions from European soils under different land use: Effects of soil moisture and temperature. *European Journal of Soil Science*, *61*(5), 683–696. https://doi.org/10.1111/j.1365-2389.2010.01277.x

Schlesinger, W. H. (2009). On the fate of anthropogenic nitrogen. *Proceedings of the National Academy of Sciences of the United States of America*, *106*(1), 203–208. https://doi.org/10.1073/pnas.0810193105

Sharp, S. J., Elgersma, K. J., Martina, J. P., & Currie, W. S. (2020). Hydrologic flushing rates drive nitrogen cycling and plant invasion in a freshwater coastal wetland model. *Ecological Applications*, *31*, e2233. https://doi.org/10.1002/eap.2233

Sierszen, M. E., Brazner, J. C., Cotter, A. M., Morrice, J. A., Peterson, G. S., & Trebitz, A. S. (2012). Watershed and lake influences on the energetic base of coastal wetland food webs across the Great Lakes Basin. *Journal of Great Lakes Research*, *38*(3), 418–428. https://doi.org/10.1016/j.jglr.2012.04.005

Sitch, S., Smith, B., Prentice, I. C., Arneth, A., Bondeau, A., Cramer, W., et al. (2003). Evaluation of ecosystem dynamics, plant geography and terrestrial carbon cycling in the LPJ dynamic global vegetation model. *Global Change Biology*, *9*(2), 161–185. https://doi.org/10.1046/j.1365-2486.2003.00569.x

Song, C., Xu, X., Tian, H., & Wang, Y. (2009). Ecosystem–atmosphere exchange of CH_4 and N_2O and ecosystem respiration in wetlands in the Sanjiang Plain, Northeastern China. *Global Change Biology*, *15*(3), 692–705. https://doi.org/10.1111/j.1365-2486.2008.01821.x

Song, Y., Linderholm, H. W., Chen, D., & Walther, A. (2010). Trends of the thermal growing season in China, 1951–2007. *International Journal of Climatology: A Journal of the Royal Meteorological Society*, *30*(1), 33. https://doi.org/10.1002/joc.1868

Søvik, A. K., Augustin, J., Heikkinen, K., Huttunen, J. T., Necki, J. M., Karjalainen, S. M., et al. (2006). Emission of the greenhouse gases nitrous oxide and methane from constructed wetlands in Europe. *Journal of Environmental Quality*, *35*(6), 2360–2373. https://doi.org/10.2134/jeq2006.0038

Stadmark, J., & Leonardson, L. (2007). Greenhouse gas production in a pond sediment: Effects of temperature, nitrate, acetate and season. *The Science of the Total Environment*, *387*(1–3), 194–205. https://doi.org/10.1016/j.scitotenv.2007.07.039

Ström, L., & Christensen, T. R. (2007). Below ground carbon turnover and greenhouse gas exchanges in a sub-arctic wetland. *Soil Biology and Biochemistry*, *39*(7), 1689–1698. https://doi.org/10.1016/j.soilbio.2007.01.019

Tan, L., Ge, Z., Zhou, X., Li, S., Li, X., & Tang, J. (2020). Conversion of coastal wetlands, riparian wetlands, and peatlands increases greenhouse gas emissions: A global meta-analysis. *Global Change Biology*, *26*(3), 1638–1653. https://doi.org/10.1111/gcb.14933

Tian, H., Xu, X., Liu, M., Ren, W., Zhang, C., Chen, G., & Lu, C. (2010). Spatial and temporal patterns of CH_4 and N_2O fluxes in terrestrial ecosystems of North America during 1979–2008: Application of a global biogeochemistry model. *Biogeosciences*, *7*(9), 2673–2694. https://doi.org/10.5194/bg-7-2673-2010

Tiedje, J. M. (1988). Ecology of denitrification and dissimilatory nitrate reduction to ammonium. *Biology of Anaerobic Microorganisms*, *717*, 179–244.

Turunen, J., Tomppo, E., Tolonen, K., & Reinikainen, A. (2002). Estimating carbon accumulation rates of undrained mires in Finland—Application to boreal and subarctic regions. *The Holocene*, *12*(1), 69–80. https://doi.org/10.1191/0959683602hl522rp

Wang, H., Liao, G., D'Souza, M., Yu, X., Yang, J., Yang, X., & Zheng, T. (2016). Temporal and spatial variations of greenhouse gas fluxes from a tidal mangrove wetland in Southeast China. *Environmental Science and Pollution Research*, *23*(2), 1873–1885. https://doi.org/10.1007/s11356-015-5440-4

Wang, H., Yu, L., Zhang, Z., Liu, W., Chen, L., Cao, G., et al. (2017). Molecular mechanisms of water table lowering and nitrogen deposition in affecting greenhouse gas emissions from a Tibetan alpine wetland. *Global Change Biology*, *23*(2), 815–829. https://doi.org/10.1111/gcb.13467

Wania, R., Ross, I., & Prentice, I. C. (2010). Implementation and evaluation of a new methane model within a dynamic global vegetation model: LPJ-WHyMe v1. 3.1. *Geoscientific Model Development*, *3*(2), 565–584. https://doi.org/10.5194/gmd-3-565-2010

Weier, K. L., Doran, J. W., Power, J. F., & Walters, D. T. (1993). Denitrification and the dinitrogen/nitrous oxide ratio as affected by soil water, available carbon, and nitrate. *Soil Science Society of America Journal*, *57*(1), 66–72. https://doi.org/10.2136/sssaj1993.03615995005700010013x

Weslien, P., Kasimir Klemedtsson, Å., Börjesson, G., & Klemedtsson, L. (2009). Strong pH influence on N_2O and CH_4 fluxes from forested organic soils. *European Journal of Soil Science*, *60*(3), 311–320. https://doi.org/10.1111/j.1365-2389.2009.01123.x

Whiting, G. J., & Chanton, J. P. (1993). Primary production control of methane emission from wetlands. *Nature*, *364*(6440), 794–795. https://doi.org/10.1038/364794a0

Whiting, G. J., & Chanton, J. P. (2001). Greenhouse carbon balance of wetlands: Methane emission versus carbon sequestration. *Tellus B: Chemical and Physical Meteorology*, *53*(5), 521–528. https://doi.org/10.3402/tellusb.v53i5.16628

Wolfe, D. W., Schwartz, M. D., Lakso, A. N., Otsuki, Y., Pool, R. M., & Shaulis, N. J. (2005). Climate change and shifts in spring phenology of three horticultural woody perennials in northeastern USA. *International Journal of Biometeorology*, *49*(5), 303–309. https://doi.org/10.1007/s00484-004-0248-9

Xu, X., Tian, H., & Hui, D. (2008). Convergence in the relationship of CO_2 and N_2O exchanges between soil and atmosphere within terrestrial ecosystems. *Global Change Biology*, *14*(7), 1651–1660. https://doi.org/10.1111/j.1365-2486.2008.01595.x

Xu, X., Zou, X., Cao, L., Zhamangulova, N., Zhao, Y., Tang, D., & Liu, D. (2014). Seasonal and spatial dynamics of greenhouse gas emissions under various vegetation covers in a coastal saline wetland in southeast China. *Ecological Engineering*, *73*, 469–477. https://doi.org/10.1016/j.ecoleng.2014.09.087

Yang, J., Liu, J., Hu, X., Li, X., Wang, Y., & Li, H. (2013). Effect of water table level on CO_2, CH_4 and N_2O emissions in a freshwater marsh of Northeast China. *Soil Biology and Biochemistry*, *61*, 52–60. https://doi.org/10.1016/j.soilbio.2013.02.009

Yvon-Durocher, G., Allen, A., Bastviken, D., Conrad, R., Gudasz, C., St-Pierre, A., et al. (2014). Methane fluxes show consistent temperature dependence across microbial to ecosystem scales. *Nature*, *507*, 488–491. https://doi.org/10.1038/nature13164

Zhang, J. B., Song, C. C., & Yang, W. Y. (2005). Cold season CH_4, CO_2 and N_2O fluxes from freshwater marshes in northeast China. *Chemosphere*, *59*(11), 1703–1705. https://doi.org/10.1016/j.chemosphere.2004.11.051

Zhou, L., Tucker, C. J., Kaufmann, R. K., Slayback, D., Shabanov, N. V., & Myneni, R. B. (2001). Variations in northern vegetation activity inferred from satellite data of vegetation index during 1981 to 1999. *Journal of Geophysical Research: Atmospheres*, *106*(D17), 20069–20083. https://doi.org/10.1029/2000JD000115

Zhu, Q., Liu, J., Peng, C., Chen, H., Fang, X., Jiang, H., et al. (2014). Modelling methane emissions from natural wetlands by development and application of the TRIPLEX-GHG model. *Geoscientific Model Development*, *7*(3), 981–999. https://doi.org/10.5194/gmd-7-981-2014